Experimental and Molecular Dynamics Simulation Study of the Sublimation and Vaporization Energetics of Iron Metalocenes. Crystal Structures of Fe(η 5 -C 5 H 4 CH 3) 2 and Fe[(η 5...

ARTICLE *in* THE JOURNAL OF PHYSICAL CHEMISTRY A · MAY 2008

Impact Factor: 2.69 · DOI: 10.1021/jp7107818 · Source: PubMed

6 AUTHORS, INCLUDING:

Jose Nuno A Canongia Lopes
Technical University of Lisbon
179 PUBLICATIONS **8,333** CITATIONS
SEE PROFILE

Maria Fatima Piedade
University of Lisbon
56 PUBLICATIONS **674** CITATIONS
SEE PROFILE

Hermínio Diogo
Technical University of Lisbon
113 PUBLICATIONS **960** CITATIONS
SEE PROFILE

Manuel E Minas da Piedade
University of Lisbon
112 PUBLICATIONS **1,547** CITATIONS
SEE PROFILE

Experimental and Molecular Dynamics Simulation Study of the Sublimation and Vaporization Energetics of Iron Metalocenes. Crystal Structures of Fe(η^5-$C_5H_4CH_3$)$_2$ and Fe[(η^5-(C_5H_5)(η^5-C_5H_4CHO)]

Cláudio M. Lousada,[†] Susana S. Pinto,[‡] José N. Canongia Lopes,[‡] M. Fátima Minas da Piedade,[†,‡] Hermínio P. Diogo,[‡] and Manuel E. Minas da Piedade*[,†]

Departamento de Química e Bioquímica, Faculdade de Ciências, Universidade de Lisboa, 1649-016 Lisboa, Portugal, and Centro de Química Estrutural, Complexo Interdisciplinar, Instituto Superior Técnico da Universidade Técnica de Lisboa, 1049-001 Lisboa, Portugal

Received: November 11, 2007; In Final Form: December 18, 2007

The standard molar enthalpies of sublimation of ferrocene, 1,1′-dimethylferrocene, decamethylferrocene, ferrocenecarboxaldehyde and α-methylferrocenemethanol, and the enthalpy of vaporization of *N*,*N*-dimethyl-(aminomethyl)ferrocene, at 298.15 K, were determined by Calvet-drop microcalorimetry and/or the Knudsen effusion method. The obtained values were used to assess and refine our previously developed force field for metallocenes. The modified force field was able to reproduce the $\Delta_{sub}H^\circ_m$ and $\Delta_{vap}H^\circ_m$ values of the test-set with an accuracy better than 5 kJ·mol^{-1}, except for decamethylferrocene, in which case the deviation between the calculated and experimental $\Delta_{sub}H^\circ_m$ values was 16.1 kJ·mol^{-1}. The origin of the larger error found in the prediction of the sublimation energetics of decamethylferrocene, and which was also observed in the estimation of structural properties (e.g., density and unit cell dimensions), is discussed. Finally, the crystal structures of Fe(η^5-$C_5H_4CH_3$)$_2$ and Fe[(η^5-(C_5H_5)(η^5-C_5H_4CHO)] at 293 and 150 K, respectively, are reported.

Introduction

The ability to predict macroscopic physical properties of a system from a limited amount of molecular information has been a long-term goal in chemistry and engineering, as it reduces the need for expensive and time-consuming experimentation. In the case of the enthalpy of sublimation of organometallic compounds this problem has barely been investigated, in spite of the fact that values of $\Delta_{sub}H^\circ_m$ are often needed, for example, to obtain metal−ligand "bond strengths" from calorimetric studies[1−3] or to design chemical vapor deposition processes.[4,5] In contrast, for organic compounds, a number of empirical estimation schemes based on various structural motifs[6−13] and correlations with physical properties (e.g., the temperature of fusion),[14] and molecular parameters (e.g., the number of valence electrons or the van der Waals surface)[15] have been reported.

The lack of experimental data[16−18] is perhaps the major obstacle in the development of empirical correlations valid for, at least, homologous series of organometallic compounds. This seems to be possible, however, as shown by the good linear relation observed by plotting the enthalpies of sublimation of M(η^5-C_5H_5)$_2$Cl$_2$ (M = Ti, Zr, Hf, V, Nb, Ta, Mo, W) compounds against the atomic radii of the metals.[19] Another problem is the large variety of combinations of metals and ligands found in organometallic species, which makes the development of general empirical estimation methods more difficult than for organic compounds.

Although not a "paper and pencil" method, such as the schemes and correlations mentioned above, a much more promising and general approach seems to be the use of atom−atom pair potential calculations.[20,21] This technique currently allows, to a considerable extent, the interpretation of packing effects in many crystals and is being intensively applied (though still with limited success)[22−24] in the investigation of the ab initio prediction of crystal structures, i.e., the prediction of crystal structures based only on the knowledge of the molecular structure.[15,21−25] It has also been used to estimate enthalpies of sublimation of organic compounds,[13,15,21] along with other computational methods, such as those based on neural networks,[13] structure activity relationships[26,27] or PIXEL integration (integral sums over the molecular electron density to obtain Coulombic, polarization, dispersion, and repulsion lattice energies).[28] Since the starting point for the prediction of $\Delta_{sub}H^\circ_m$ by the atom−atom method is the knowledge of the crystal structure of the compound of interest, the method does in principle allow for the discrimination between different polymorphs, which represents a considerable advantage over empirical procedures.

A key aspect for the application of the atom−atom method is the definition of an intermolecular potential function capable of accurately describing the interactions that simultaneously determine the enthalpy of sublimation and the structure of the crystal. Various potential functions and parametrizations have been developed, mainly for organic molecules, from statistical analysis of reported structure and enthalpy of sublimation data.[20−22,25,29] In the case of organometallic compounds, an ample structural databank is available[30] but, as mentioned above, very little information exists on enthalpies of sublimation.[16−18] Moreover, since the characterization of the solid samples in terms of phase purity has been overlooked in most experimental measurements of $\Delta_{sub}H^\circ_m$, there are very few data that can safely be assigned to a definite crystal structure and used as accurate benchmarks to validate the calculations.

This led us to embark on a systematic experimental and computational study of the quantitative relation between structure and enthalpy of sublimation in organometallic compounds.

* Author to whom correspondence should be addressed. E-mail: memp@fc.ul.pt.
[†] Universidade de Lisboa.
[‡] Instituto Superior Técnico da Universidade Técnica de Lisboa.

10.1021/jp7107818 CCC: $40.75
Published on Web 03/11/2008

In a previous report a simple but transferable force field for metallocenes, integrated with the OPLS-AA model, was developed and shown to correctly capture the volumetric properties of a number of solid ferrocene derivatives.[31] Although primarily developed for solids, the model did not incorporate any restrictions regarding liquids. Hence its application to the prediction of the sublimation and vaporization energetics was investigated in this work. The results of the computations were assessed, and the model was refined using the enthalpies of sublimation of the solid compounds **1**−**5** and the enthalpy of vaporization of **6**, determined by Calvet-drop microcalorimetry and/or the Knudsen effusion method.

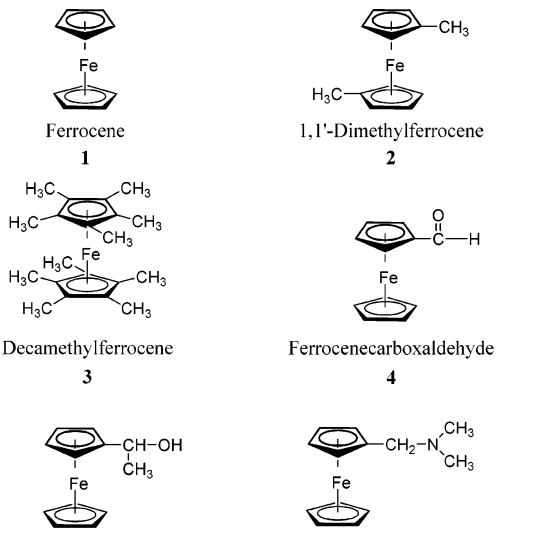

Materials and Methods

General. Elemental analyses (C, H) were made on a Fisons Instruments EA1108 apparatus, with typical maximum accuracy errors of ±0.3% for carbon and ±0.1% for hydrogen. IR spectra were carried out on Jasco 430, Jasco 4100, or Mattson satellite spectrophotometers, calibrated with polystyrene film. ^{1}H NMR spectra were obtained using a Varian Gemini 200 (300 MHz) or a Bruker Ultrashield (400 MHz) spectrometer. Mass spectra were recorded on a Fisons Instruments Trio 1000 apparatus. X-ray powder diffractograms (XRD) were obtained at 293 ± 2 K, using Cu Kα radiation, on D8 Bruker AXS, Philips PW1710, or Rigaku Geigerflex diffractometers. The data were collected over the range $5° \le 2\theta \le 35$ °, with a scan speed of 0.5° (2θ ·min^{-1}), and a step size 0.020° (2θ). The indexation of the powder patterns was performed using the program Checkcell.[32] Differential scanning calorimetry (DSC) experiments were made with a temperature-modulated TA Instruments 2920 MTDSC apparatus, operated as a conventional DSC. The samples were sealed under air in aluminum pans, and weighed to ± 10^{-7} g on a Mettler UMT2 ultra-microbalance. Helium (Air Liquide N55) at a flow rate of 0.5 cm^3·s^{-1} was used as the purging gas. The temperature and heat flow scales of the instrument were calibrated as previously described.[33]

Materials. Fe(η^5-C_5H_5)$_2$. Ferrocene ([CAS 102-54-5] Aldrich 98%) was purified by sublimation at 328 K and 5.3 Pa prior to use. Elemental analysis for $C_{10}H_{10}Fe$: expected C 64.56%, H 5.42%; found C 64.53%, H 5.39% (average of two determinations). FT-IR (KBr, main peaks): $\tilde{\nu}$/cm^{-1} = 3083 (ν_{C-H}, C_5H_5); 1105, 1408 (ν_{C-C}, C_5H_5); 1001 (δ_{C-H}, C_5H_5); 815, 850 (π_{C-H}, C_5H_5); 475 ($\nu_{Fe-C_5H_5}$). The assignments were based on those given by Nakamoto.[34] ^{1}H NMR (400 MHz, $CDCl_3$/TMS): δ = 4.173 (s, 10H, C_5H_5). The ^{1}H NMR results are in agreement with those reported in a reference database.[35] The powder pattern was indexed as monoclinic, space group $P2_1/a$, with a = 10.505(6) Å, b = 7.589(9) Å, c = 5.912(6) Å, β = 120.9(6)°. These values are in good agreement with a = 10.530(8) Å, b = 7.604(5) Å, c = 5.921(4) Å, β = 121.0(6)° previously obtained by neutron diffraction.[36] The onset (T_{on}) and the maximum (T_{max}) temperature of the melting peak, obtained by DSC at a scan rate of 5 K·min^{-1}, were T_{on} = 447.73 ± 0.12 K and T_{max} = 448.51 ± 0.07 K, respectively and the corresponding enthalpy of fusion $\Delta_{fus}H^\circ_m$ = 17.81 ± 0.06 kJ·mol^{-1}. The uncertainties quoted are twice the standard deviation of the mean of four determinations. The samples had masses in the range of 4.2−6.2 mg. The previously reported enthalpies of fusion of ferrocene are in the range 17.8−18.5 kJ·mol^{-1}.[37−39]

Fe(η^5-$C_5H_4CH_3$)$_2$. 1,1′-Dimethylferrocene (CAS [1291-47-0], Aldrich 97%) was purified by sublimation at 296 K and 2.2 Pa prior to use. Elemental analysis for $C_{12}H_{14}Fe$: expected C 67.32%, H 6.59%; found C 67.52%, H 7.06% (average of two determinations). FT-IR (KBr, main peaks): $\tilde{\nu}$/cm^{-1} = 3077 (ν_{C-H}, C_5H_5); 2966, 2944, 2919 (ν_{C-H}, CH_3); 2881, 1772, 1749, 1729, 1698, 1683, 1651; 1474, 1462 (symmetric bending CH_3); 1379 (asymmetric bending CH_3); 1359 (ν_{C-C}, in-plane skeletal vibration); 1226 (ν_{C-CH_3}); 1054, 1037 (δ_{C-H}); 1024 (ring breathing); 924, 918; 850 (δ_{C-C}); 811 (out-of-plane bend π_{C-H} perpendicular); 633, 602 (δ_{C-C}); 502 (asymmetric $\nu_{Fe-C_5H_5CH_3}$); 479 (asymmetric $\delta_{Fe-C_5H_5CH_3}$). The assignments were based on those given by Phillips et al.[40] ^{1}H NMR (300 MHz, $CDCl_3$/TMS): δ = 1.935 (s, 6H, CH_3); 3.990 (s, 8H, C_5H_4), in good agreement with previously reported data.[41] The powder pattern was indexed as monoclinic, space group $P2_1/c$, with a = 12.236(4) Å, b = 7.483(6) Å, c = 10.803(4) Å, β = 103.6(5)°. These values are in agreement with a = 12.334(6) Å, b = 7.526(3) Å, c = 10.954(4) Å, β = 102.81(2) obtained in this work at 293 K by single-crystal X-ray diffraction. The onset and the maximum temperature of the melting peak, obtained by DSC at a scan rate of 10 K·min^{-1}, were T_{on} = 311.55 ± 0.11 K and T_{max} = 312.60 ± 0.21 K, respectively, and the corresponding enthalpy of fusion $\Delta_{fus}H^\circ_m$ = 17.66 ± 0.06 kJ·mol^{-1}. The uncertainties quoted are twice the standard deviation of the mean of four determinations. The samples had masses in the range 3.8 mg to 4.9 mg.

Fe[η^5-$C_5(CH_3)_5$]$_2$. Decamethylferrocene (CAS [12126-50-0], Aldrich 97%) was purified by sublimation at 413 K and 5.3 Pa. Elemental analysis for $C_{20}H_{30}Fe$: expected C 73.62%, H 9.27%; found C 73.42%, H 9.12% (average of two determinations). FT-IR (KBr, main peaks): $\tilde{\nu}$/cm^{-1} = 2965, 2945, 2896 (ν_{C-H}, CH_3); 1377, 1373 (symmetric bending CH_3); 1473, 1449, 1426 (asymmetric bending CH_3); 1356 (ν_{C-C}, in-plane skeletal vibration); 587 (ring breathing); 453 (asymmetric $\nu_{Fe-C_5H_5CH_3}$). These results agree with those published by Stanghellini and co-workers.[42] ^{1}H NMR (300 MHz, $CDCl_3$/TMS): δ = 1.63 (s, 30H, $C_5(CH_3)_5$). The powder pattern was indexed as orthorhombic space group C_{mca}, a = 15.238(6) Å, b = 11.919(5) Å, c = 9.862(9) Å. These values are in agreement with a = 15.210(3) Å, b = 11.887(2) Å, c = 9.968(2) Å, obtained by single-crystal X-ray diffraction.[43] Two endothermic events, corresponding to solid−solid phase transitions were detected before fusion, by DSC. For the first transition T_{on} = 401.11 ± 0.05 K, T_{max} = 402.55 ± 0.04 K and $\Delta_{trs}H^\circ_m$ = 4.30 ± 0.04 kJ·mol^{-1}; for the second transition T_{on} = 503.12 ± 0.11 K, T_{max} = 503.74 ± 0.08 K, and $\Delta_{trs}H^\circ_m$ = 4.87 ± 0.05 kJ·mol^{-1}. Fusion occurred with partial decomposition of the sample at T_{on} =

576.89 ± 0.15 K and T_{max} = 577.32 ± 0.09 K (average of two determinations). The DSC experiments were carried out at a scan rate of 5 K·min^{-1} using masses of sample in the range 3.5 mg to 6.6 mg.

Fe[(η^5-C_5H_5)(η^5-C_5H_4CHO)]. Ferrocenecarboxaldehyde (CAS [12093-10-6], Aldrich 98%) was purified by sublimation at 298 K and 1.1 Pa. Elemental analysis for $C_{11}H_{10}OFe$: expected C 61.73%, H 4.71%; found C 61.51%, H 4.56% (average of two determinations). FT-IR (KBr, main peaks): $\tilde{\nu}$/cm^{-1} = 3087 (ν_{C-H}, C_5H_5); 2866, 2833, 2804, 2762, 2727 (ν_{C-H}, CHO); 1680 (ν_{C-O}, CHO); 1105, 1410 (ν_{C-C}, C_5H_5); 1388 (δ_{C-H}, CHO); 1001 (δ_{C-H}, C_5H_5); 823, 841 (π_{C-H}, C_5H_5); 498 (C_5H_5 ring tilt); 480 ($\nu_{Fe-C_5H_5}$). ^{1}H NMR (400 MHz, $CDCl_3$/TMS): δ = 4.271 (5H, C_5H_5), 4.604 (2H, C_5H_4), 4.791 (2H, C_5H_4), 9.949 (1H, CHO). The observed FT-IR and ^{1}H NMR spectra are in good agreement with those indicated in a reference database.[35] The X-ray powder pattern was indexed as orthorhombic, space group $P2_12_12_1$, with a = 7.597(7) Å, b = 10.448(4) Å, c = 11.241(3) Å. These values are in agreement with those previously reported from single-crystal X-ray diffraction experiments carried out at room temperature a = 7.639(5) Å, b = 10.525(8) Å, c = 11.294(10) Å.[44] A solid−solid phase transition with $\Delta_{trs}H^\circ_m$ = 11.6 ± 0.3 kJ·mol^{-1}, was observed by DSC at T_{on} = 316.2 ± 0.2 K and T_{max} = 317.4 ± 0.3 K. This was followed by fusion at T_{on} = 396.6 ± 0.2 K, T_{max} = 397.2 ± 0.2 K, for which $\Delta_{fus}H^\circ_m$ = 2.5 ± 0.2 kJ·mol^{-1}. The uncertainties quoted are twice the standard deviation of the mean of four determinations. The obtained values are in good agreement with the DSC results previously reported by Daniel et al. (T_{trs} = 316.4 K; $\Delta_{trs}H^\circ_m$ = 11.7 ± 0.3 kJ·mol^{-1}, T_{fus}= 396.7 K, $\Delta_{fus}H^\circ_m$= 2.05 ± 0.06 kJ mol^{-1})[45] and in reasonable agreement with the more recent adiabatic calorimetry determinations by Kaneko and Sorai (T_{trs} = 317.03 K; $\Delta_{trs}H^\circ_m$ = 13.29 ± 0.10 kJ·mol^{-1}, T_{fus}= 397.60 K, $\Delta_{fus}H^\circ_m$ = 2.76 kJ mol^{-1}).[46] The experiments were carried out at a scan rate of 5 K·min^{-1}, using samples with masses in the range of 3.3−6.7 mg.

Fe[(η^5-C_5H_5)(η^5-$C_5H_4CHCH_3OH$)]. α-Methylferrocenemethanol (CAS [1277-49-2], Aldrich 97%; racemic mixture) was purified by sublimation at 310 K and 1.5 Pa, followed by recrystallization from petroleum ether 40−60°. Elemental analysis for $C_{12}H_{14}OFe$: expected C 62.65%, H 6.13%; found C 62.86%, H 6.08% (average of two determinations). FT-IR (KBr, main peaks): $\tilde{\nu}$/cm^{-1} = 3924 (ν_{C-H}, C_5H_5); 3213, 3088, 2973, 2930, 1635, 1410, 1363, 1307, 1237, 1105, 1068, 1000 (δ_{C-H}, C_5H_5); 917, 869, 807 (π_{C-H}, C_5H_5); 511 (C_5H_5 ring tilt); 482, 4366 ($\nu_{Fe-C_5H_5}$). ^{1}H NMR (400 MHz, $CDCl_3$/TMS): δ = 4.548 (m, 1H, CH), 4.197 (m, 9H, C_5H_4 and C_5H_5), 1.823 (d, 2H, OH), 1.432 (d, 3H, CH_3). The observed ^{1}H NMR spectrum is in good agreement with that reported in the literature.[47] The X-ray powder pattern was indexed as tetragonal, space group $I4_1cd$, with $a = b$ = 23.293(0) Å, c = 7.710(2) Å. These values are in agreement with those obtained by single-crystal X-ray diffraction $a = b$ = 23.3334(18) Å, c = 7.7186(11) Å.[48] The onset and the maximum temperature of the fusion peak obtained by DSC at a scan rate of 5 K·min^{-1} were T_{on} = 335.56 ± 0.11 K and T_{max} = 343.71 ± 0.09 K, respectively, and the corresponding enthalpy of fusion $\Delta_{fus}H^\circ_m$ = 14.75 ± 0.06 kJ·mol^{-1}. The uncertainties quoted are twice the standard deviation of the mean of four determinations. The samples had masses in the range of 5.2−7.1 mg.

Fe[(η^5-C_5H_5){η^5-$C_5H_4CH_2N(CH_3)_2$}]. *N*,*N*-Dimethyl(aminomethyl)ferrocene (CAS [1271-86-9], Aldrich 96%, ρ = 1.228 g·cm^{-3}) was purified by distillation at 373 K and 1.1 Pa. FT-IR (NaCl windows, main peaks): $\tilde{\nu}$/cm^{-1} = 3092, 2966, 2937, 2854, 2813, 2764, 2720, 1685, 1467, 1455, 1438, 1412, 1380, 1348, 1260, 1231, 1171, 1136, 1105, 1039, 1021, 1001, 928, 843. ^{1}H NMR (400 MHz, $CDCl_3$/TMS): δ = 4.15 (5H, C_5H_5); 4.10 (4H, C_5H_4), 3.26 (2H, R_2NCH_2Cp), 2.16 (6H, $(H_3C)_2N-$). Mass spectrum (70 eV, sample temperature 302 K, source temperature 523 K): *m*/*z* (relative intensities) = 244 (10.93), 243 (67.33), 242 (22.57), 241 (9.50), 201 (3.67), 200 (23.49), 199 (86.50), 197 (9.69), 187 (2.73), 186 (27.27), 178 (4.13), 177 (4.12), 175 (8.29), 163 (20.40), 162 (29.44), 135 (10.34), 134 (14.64), 129 (5.65), 122 (16.17), 121 (100.0), 119 (11.93), 106 (5.88), 99 (7.92), 97 (5.37), 95 (6.86), 94 (12.45), 83 (3.00), 81 (8.97), 79 (6.46), 78 (12.78), 77 (11.94), 65 (5.89), 58 (21.80), 56 (49.48), 44 (6.05), 42 (26.20). The observed FT-IR, ^{1}H NMR and mass spectra are in good agreement with those indicated in a reference database.[35] The onset and the maximum temperatures of the fusion peak obtained by DSC, using samples with masses in the range of 2.9−5.8 mg and a scan rate of 5 K·min^{-1}, were T_{on} = 278.40 ± 0.13 K and T_{max} =281.46 ± 0.09 K, respectively, and the corresponding enthalpy of fusion $\Delta_{fus}H^\circ_m$ = 14.6 ± 0.2 kJ·mol^{-1}. The uncertainties quoted are twice the standard deviation of the mean of four determinations. These results are in reasonable agreement with the previously reported T_{fus} = 280.94 ± 0.01 K and $\Delta_{fus}H^\circ_m$ = 15.01 ± 0.02 kJ·mol^{-1}.[49]

Single-Crystal X-ray Diffraction. Single-crystal X-ray diffraction analysis of dimethylferrocene was performed at 293 K on a MACH3 Enraf-Nonius diffractometer equipped with Mo Kα radiation (λ = 0.710 73 Å). Data were corrected for Lorentz and polarization effects, and for absorption, using the DIFABS empirical method included in WINGX-Version 1.70.01.[50] Data collection and data reduction were done with the CAD4 and XCAD programs.[51] In the case of ferrocenecarboxaldehyde the analysis was carried out at 150 K on a Bruker AXS APEX CCD area detector diffractometer, using graphite-monochromated Mo Kα (λ = 0.710 73 Å) radiation. Intensities were corrected for Lorentz polarization effects. An empirical absorption correction was applied using SADABS,[52] and the data reduction was done with the SMART and SAINT programs.[53] All structures were solved by direct methods with SIR97[54] and refined by full-matrix least-squares on F^2 using SHELXL97,[55] both included in WINGX-Version 1.70.01.[50] Non-hydrogen atoms were refined with anisotropic thermal parameters whereas H atoms were placed in idealized positions and allowed to refine riding on the parent C atom. Graphical representations were prepared using ORTEP[56] and Mercury 1.1.2.[57] The PARST program[58] was used to calculate intermolecular interactions in both cases. A summary of the crystal data, structure solution and refinement parameters is given in Table 1.

Knudsen Effusion Experiments. The Knudsen effusion apparatus used to determine the enthalpies of sublimation of Fe(η^5-C_5H_5)$_2$, Fe(η^5-$C_5H_4CH_3$)$_2$, Fe[η^5-$C_5(CH_3)_5$]$_2$, and Fe[(η^5-C_5H_5)(η^5-C_5H_4CHO)] has been previously described.[19,59,60] The effusion holes were drilled in a 2.090 × 10^{-5} m thick copper foil (Cu 99%, Goodfellow Metals) soldered to the cell lid and had areas of 6.952 × 10^{-7} m^2 (hole 1; ferrocene), 4.390 × 10^{-7} m^2 (hole 2; 1,1′-dimethylferrocene, and decamethylferrocene), and 6.910 × 10^{-7} m^2 (hole 3; ferrocenecarboxaldehyde). In the case of Fe(η^5-C_5H_5)$_2$, Fe(η^5-$C_5H_4CH_3$)$_2$, and Fe[(η^5-(C_5H_5)(η^5-C_5H_4CHO)] this block was immersed in a water bath whose temperature was controlled to ±0.01 K with a Haake ED Unitherm thermostat and measured with the same precision with a calibrated mercury thermometer. A Haake EK12 cryostat was used as a heat sink. In the experiments with Fe[η^5-$C_5(CH_3)_5$]$_2$ the water bath was replaced by a tubular furnace surrounding

TABLE 1: Crystal Data and Structure Refinement for 1,1′-Dimethylferrocene and Ferrocenecarboxaldehyde

	$Fe(\eta^5\text{-}C_5H_4CH_3)_2$	$Fe[(\eta^5\text{-}C_5H_5)\text{-}(\eta^5\text{-}C_5H_4CHO)]$
empirical formula	C12 H14 Fe	C11 H10 Fe O
formula weight	214.08	214.04
T/K	293(2) K	150(1) K
wavelength/Å	0.71073	0.71073
crystal size/mm	0.17 × 0.15 × 0.11	0.2 × 0.2 × 0.2
color of crystal	orange	red
crystal system	monoclinic	orthorhombic
space group	$P2_1/a$	$P2_12_12_1$
a/Å	10.954(4)	7.639(6)
b/Å	7.526(3)	10.518(8)
c/Å	12.334(6)	11.300(9)
β/deg	102.81(2)	
V/Å^3	991.5(7)	907.9(12)
Z	4	4
ρ_{calcd}/g·cm^{-3}	1.434	1.566
μ/mm^{-1}	1.467	1.610
F(000)	448	440
θ limits/deg	1.69 − 25.07	2.65 − 28.37
limiting indices	$0 \le h \le 12$ $0 \le k \le 8$ $-14 \le l \le 14$	$-10 \le h \le 9$ $-14 \le k \le 11$ $-15 \le l \le 14$
reflns collected/unique	1675/1675 [*R*(int) = 0.0000]	5487/2246 [*R*(int) = 0.0576]
completeness to *θ*	95.5% (*θ* = 25.07)	99.2% (*θ* = 28.37)
refinement method	full-matrix least-squares on F^2	full-matrix least-squares on F^2
data/restraints/params	1675/0/118	2246/1/118
GOF on F^2	1.023	1.000
final *R* indices [$I > 2\sigma(I)$]	$R_1 = 0.0798$	$R_1 = 0.0541$
R indices (all data)	$R_1 = 0.1041$	$R_1 = 0.0988$
absolute structure param		0.10(6)
largest diff peak and hole/e·Å^{-3}	1.221 and −1.114	0.456 and −0.338

the brass block. The temperature was controlled to better than ±0.1 K, by a Eurotherm 902P thermostatic unit, and a K type thermocouple placed in contact with the inner wall of the furnace. The temperature of the brass block was measured with a precision of ±0.1 K by a Tecnisis 100 Ω platinum resistance thermometer embedded in the block and connected in a four wire configuration to a Keithley 2000 multimeter. The equilibrium temperature inside the cell was assumed to be identical to the temperature of the water bath or of the brass block, respectively. The cells were initially charged with ca. 0.2−0.5 g of sample, and the mass loss in each run was determined to ±10^{-5} g with a Mettler AT201 balance.

Calvet Microcalorimetry. The enthalpies of sublimation of $Fe(\eta^5\text{-}C_5H_5)_2$, $Fe(\eta^5\text{-}C_5H_4CH_3)_2$, $Fe[(\eta^5\text{-}C_5H_5)(\eta^5\text{-}C_5H_4CHO)]$ and $Fe[(\eta^5\text{-}(C_5H_5)(\eta^5\text{-}C_5H_4CHCH_3OH)]$, and the enthalpy of vaporization of $Fe[(\eta^5\text{-}C_5H_5)\{\eta^5\text{-}C_5H_4CH_2N(CH_3)_2\}]$ were also measured by using the electrically calibrated Calvet microcalorimeter and the operating procedure previously reported.[61,62] In a typical experiment the sample with a mass in the range 2−22 mg was placed into a small glass capillary and weighed with a precision of 1 μg in a Mettler M5 microbalance. The capillary was equilibrated for ca. 10 min, at $T = 298.15$ K, inside a furnace placed above the entrance of the calorimetric cell, and subsequently dropped into the cell under N_2 atmosphere. The temperature of the calorimetric cell was set to 298.15 K for $Fe(\eta^5\text{-}C_5H_5)_2$ and $Fe(\eta^5\text{-}C_5H_4CH_3)_2$, 311.2 K for $Fe[(\eta^5\text{-}C_5H_5)\text{-}(\eta^5\text{-}C_5H_4CHO)]$, 311.0 K for $Fe[\eta^5\text{-}C_5H_5)(\eta^5\text{-}C_5H_4CHCH_3OH)]$, and 305.1 K for $Fe[(\eta^5\text{-}C_5H_5)\{\eta^5\text{-}C_5H_4CH_2N(CH_3)_2\}]$. After dropping, an endothermic peak due to the heating of the sample from room temperature to the temperature of the calorimeter was first observed. When the signal returned to the baseline the sample and reference cells were simultaneously evacuated to 1.3 × 10^{-4} Pa and the measuring curve corresponding to the vaporization or sublimation of the compound was acquired. The corresponding enthalpy of sublimation or vaporization was subsequently derived from the area of the obtained curve and the calibration constant of the apparatus. No decomposition residues were found inside the calorimetric cell at the end of the experiments.

Density Functional Theory Calculations. Density functional theory calculations were carried out with the Gaussian-03 program.[63] The geometries were fully optimized and the total energies were calculated using the Becke's three-parameter hybrid method[64] with the Perdew and Wang PW91[65] correlation functional (B3PW91) and the SDDall basis set (SDD effective core potentials and triple-ζ valence basis sets on all heavy atoms and D95 for hydrogens).[66,67] In previous tests the B3PW91/SDDall model proved to be a reliable, economical, and practical approach to obtain accurate geometrical data for ferrocene derivatives.[31] All the total energies, given as Supporting Information, were corrected with the zero-point vibration energies calculated at the same theoretical level. Atomic point charges (ESP charges) were determined at the BPW91/6-311G-(3df,3pd) level of theory, through a fit to the molecular electrostatic potential, using the CHelpG procedure[68] and the BPW91/SDDall equilibrium geometry.

Molecular Dynamics (MD) Simulations. The molecular dynamics runs were performed using the DL_POLY package[69] and a refined version of the previously reported all-atom force field developed to model ferrocene and its derivatives within the framework of the OPLA_AA parametrization.[31] In the former version of the force field the five carbon atoms of the cyclopentadienyl (Cp) ring and the five atoms attached to them (either hydrogens or the atoms from substituents directly involved in the bond to the Cp ring) were considered as a rigid unit. The remaining fragments of the ring substituents were modeled using the corresponding OPLS-AA (or AMBER) bond, angle, dihedral and improper dihedral constraints. This was subsequently found to lead to convergence problems during the simulation of some ferrocene derivatives. To overcome this problem, it was assumed in the present refinement of the force field that the five "backbone" carbon atoms of the Cp ring still form a rigid unit but all Cp ring substituents (any atom attached directly or indirectly to the backbone carbon atoms) are modeled using the usual OPLS-AA (or AMBER) parameters.[70−73] The only other departure from the previously reported force field[31] was related to the nonbonded interactions (Lennard-Jones parameters) of the iron atom. Preliminary simulations using the whole Cp ring as a rigid unit yielded $\Delta_{sub}H^\circ_m[Fe(\eta^5\text{-}C_5H_5)_2] = 76 \pm 3$ kJ·mol^{-1} at 298.15 K,[31] in good agreement with the recommended value of 73.48 ± 1.08 kJ·mol^{-1} for the use of ferrocene as a standard reference material for enthalpy of sublimation measurements.[17,74] However, when the constraint of rigid Cp substituents was waived, significant overestimations of the standard molar enthalpy of sublimation of ferrocene and other ferrocene-derivatives were observed. A closer inspection at the parameters used for the iron atom in the nonrefined force field showed that the nonbonded interaction parameter ϵ (that was adapted from a Buckingham-type potential fitted to simulation data performed on a rigid ferrocene model)[75] was too high in the context of the OPLS-AA framework, particularly when only the backbones of the metallocene molecules were modeled as rigid units. We therefore decided to modify the ϵ parameter for iron in order to match the simulation results with the average of the experimental values for the standard molar enthalpy of sublimation of ferrocene obtained in this work by

Knudsen effusion and Calvet microcalorimetry (73 kJ·mol^{-1}, see below). The new value of ϵ for the iron atom, used in all simulations reported in this paper, is 1.2 kJ·mol^{-1}. It must be stressed that the decision of using the ϵ parameter for iron as a fitting variable, and retain the OPLS-AA parameters for all other atoms, was based on the rationale behind the development of the present force-field:[31] a model for the prediction of the properties of organometallic compounds that is compatible with the OPLS-AA parametrization for their organic fragments.

The condensed phases were modeled as boxes containing a number of molecules ranging from 144 (decamethylferrocene) to 280 (ferrocene), which correspond to an average number of atoms of around 6000 and to cutoff distances of 1.6 nm. The Ewald summation technique was used to account for long-range interactions beyond those cutoffs. In the case of the solid compounds, the simulation boxes and initial configurations were set taking into account the dimensions and occupancy of the unit cells of the crystalline structures at various temperatures selected from the Cambridge Structural Database (CSD)[30] (ferrocene CSD ref codes, FEROCE04-06, 13, 24, 27, 29, 31;[36,76−78] 1,1′-dimethylferrocene CSD ref code, ZAYDUY;[79] decamethylferrocene CSD ref code, DMFERR01;[43] ferrocenecarboxaldehyde CSD ref code, DEJZAT;[44] α-methylferrocenemethanol CSD ref code, HIDXOH[48]) or obtained in this work for 1,1′-dimethylferrocene and ferrocenecarboxaldehyde. Since the dimensions of the unit cells of the crystals were too small to accommodate a sufficiently large cutoff distance, well-proportioned simulation boxes consisting of several stacked cells were used. The simulations were performed under the anisotropic isothermal−isobaric ensemble (*N*-σ-*T*) at 298 K and 0.1 MPa and typical runs consisted of an equilibration period of ca. 100 ps followed by production stages of 400 ps. Other details concerning the simulation of crystalline structures using an OPLS-based force field can be found elsewhere.[31,80] In the case of the liquid *N*,*N*-dimethyl(aminomethyl)ferrocene, 200 molecules were randomly placed in a large cubic box (using an expanded cubic lattice to avoid superimposition) and the system was allowed to evolve for more than 500 ps under isotropic isothermal−isobaric ensemble (*N*-*p*-*T*) conditions, to its equilibrium density at 298 K and 0.1 MPa. The final size of the box allowed a cutoff distance of 1.6 nm. For all compounds, the vapor phase was modeled *via* isolated molecules in the canonical (*N*-*V*-*T*) ensemble at 298 K. Since the statistics are poor due to the small number of atoms, each production run took 40 ns and 20 such runs were used to calculate the average gas-phase properties.

Results and Discussion

The standard atomic masses recommended by the IUPAC Commission in 2005[81] were used in the calculation of all molar thermochemical quantities.

Molecular and Crystal Structure Determination. The bond distances and angles obtained by single-crystal X-ray diffraction for Fe(η^5-$C_5H_4CH_3$)$_2$ at 293 K and Fe[(η^5-C_5H_5)(η^5-C_5H_4CHO)] at 150 K are given in Table 2. A comparison of some selected geometrical features of both compounds found in this work, with the corresponding information previously reported at different temperatures, is presented in Table 3.

The crystal structure of Fe(η^5-$C_5H_4CH_3$)$_2$ at 293 K consists of four molecules per unit cell. A perspective representation of the compound is shown in Figure 1, along with the labeling scheme used. Similarly to what has been found by Foucher et al.[79] at 173 K, the cyclopentadienyl rings are almost eclipsed and the methyl substituents are in the *cis* conformation.

TABLE 2: Bond Lengths (Å) and Angles (deg) for 1,1′-Dimethylferrocene and Ferrocenecarboxaldehyde

	Fe(η^5-$C_5H_4CH_3$)$_2$	Fe[(η^5-C_5H_5)-(η^5-C_5H_4CHO)]
Fe(1)−Cp2	1.6447(10)	1.6380(11)
Fe(1)−Cp1	1.6487(10)	1.6523(11)
Fe(1)−C(Cp)	2.011(7)−2.062(7)	2.007(6)−2.049(5)
C(1)−C(2)	1.386(10)	1.411(11)
C(3)−C(2)	1.398(10)	1.390(9)
C(4)−C(3)	1.440(10)	1.366(8)
C(4)−C(5)	1.411(11)	1.390(9)
C(1)−C(5)	1.436(9)	1.400(11)
C(6)−C(7)	1.407(11)	1.402(10)
C(7)−C(8)	1.396(12)	1.390(12)
C(8)−C(9)	1.403(11)	1.404(13)
C(10)−C(9)	1.426(9)	1.350(12)
C(6)−C(10)	1.425(10)	1.382(9)
C(6)−C(11)		1.444(14)
O(11)−C(11)		1.042(10)
C(5)−C(51)	1.474(9)	
C(10)−C(101)	1.530(10)	
Cp(1)−Fe(1)−Cp(2)	178.47(6)	178.86(5)
O(11)−C(11)−C(6)		142.5(17)

However, the Fe−$Cp_{centroid}$ bond distances as well as the Fe−C_{Cp} lengths presently obtained at 293 K are somewhat smaller than those reported at 173 K: 1.6447 Å and 1.6487 Å at 293 K vs 1.650 Å and 1.649 Å at 173 K, respectively. This effect was also observed by Seiler and Dunitz[82] for ferrocene structures determined at different temperatures. The two C_{Cp}−C_{methyl} bond distances in the present structure are fairly different (1.474 Å and 1.530 Å) to better accommodate the bulky methyl groups. This difference is also present, although to a less extent in Foucher's structure (1.491 Å and 1.501 Å). The larger asymmetry of the C_{Cp}−C_{methyl} bond distances at 293 K is probably due to the increase of the thermal motion of the atoms with the temperature. The crystal of 1,1′-dimethylferrocene is a van der Waals crystal where specific highly directional, intermolecular interactions are absent.

The ferrocenecarboxaldehyde compound is enantiomerically pure and crystallizes in the chiral space group $P2_12_12_1$. As shown in Figure 2, the cyclopentadienyl rings have an almost eclipsed conformation. Analogously to what has been found in this work for Fe(η^5-$C_5H_4CH_3$)$_2$ and by Seiler and Dunitz[82] for ferrocene, the structure of ferrocenecarboxaldehyde obtained here at 150 K exhibits longer Fe−$Cp_{centroid}$ and Fe−C_{Cp} bond distances than that reported by Daniel et al.[83] at room temperature (Table 3). The CHO substituent is almost coplanar with the Cp ring (4.6°), thus allowing conjugation of the $\pi\pi$-electron systems of the C═O bond and of the aromatic cyclopentadienyl ring. This is also observed in the published room-temperature structure.[83] The existence of CO−Cp conjugation is supported by the C(6)−C(11) bond length of 1.444 Å, which is between typical values for single and double C(6)−C(11) bond distances (1.54 Å and 1.40 Å respectively). The C═O bond length is 1.042 Å and the C(6)−C(11)−O(11) bond angle is 142.5°. In the crystal packing the CO group forms two intermolecular interactions, which are approximately of the same length: C(5)−H(5)···O(11) 2.713(7) Å and C(8)−H(8)···O(18) 2.779(7) Å. This conclusion is based on the criterion that the sum of the van der Waals radii of H and O is the higher limit for the existence of an H···O interaction.[57] The C(5)−H(5)···O(11) interaction generates a chain of molecules along the *a*-axis (Figure 3a) while the C(8)−H(8)···O(18) interaction produces another chain along the *b*-axis (Figure 3b). These two supramolecular motifs are connected making a three-dimensional network.

TABLE 3: Geometrical Parameters of the Structures of 1,1′-Dimethylferrocene and Ferrocenecarboxaldehyde Obtained at Different Temperatures

	$Fe(\eta^5\text{-}C_5H_4CH_3)_2$ ($T = 293$ K)[a]	$Fe(\eta^5\text{-}C_5H_4CH_3)_2$ ($T = 173$ K)[b]	$Fe[(\eta^5\text{-}C_5H_5)(\eta^5\text{-}C_5H_4CHO)]$ ($T = 150$ K)[a]	$Fe[(\eta^5\text{-}C_5H_5)(\eta^5\text{-}C_5H_4CHO)]$ ($T =$ room)[c]
		Bond Distance/Å		
C−C	1.386−1.440	1.403−1.433	1.350−1.411	1.371−1.430
Fe−C(Cp)	2.011−2.062		2.007−2.049	2.020−2.044
Fe−Cp	1.6447, 1.6487	1.649, 1.650	1.6380, 1.6523	
$C-C_{methyl}$	1.474−1.530	1.491, 1.501		
$C-C_{ald}$			1.444	1.481
$C_{ald}-O$			1.042	1.047
		Bond Angle/deg		
C−C−C(ring Cp)	105.1−110.3	106.6−109.0	106.2−109.3	106.7−109.8
$C-C-C_{methyl}$	125.9−127.9	125.8−127.3		
$C-C_{ald}-O$			142.5	135.8
		Dihedral Angle/deg		
$C-C-C-C_{methyl}$	178.1−179.0	176.7−177.9		
$C-C-C_{ald}-H_{ald}$				1
$C-C-C_{ald}-O_{ald}$				7
tilt angle[d]	1.49, 0.73	2.66	4.46	5.2

[a] This work. [b] Reference 79. [c] Reference 83. [d] The tilt angle is defined as the angle that the substituent ($C-C_{substituent}$) makes with the carbon plane of the substituent Cp ring.

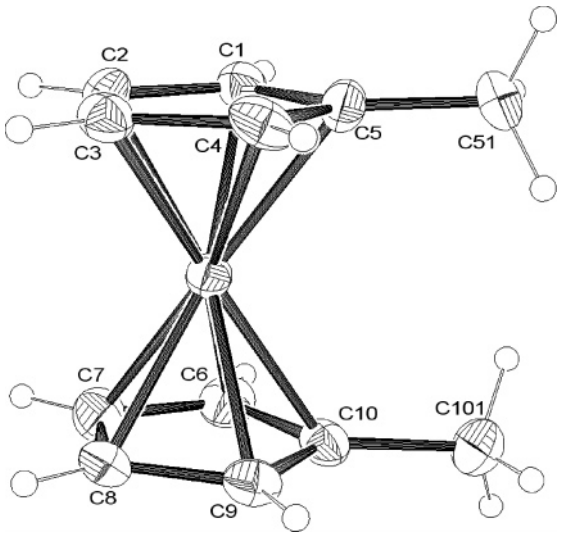

Figure 1. Molecular structure and atomic labeling scheme for 1,1′-dimethylferrocene with 50% anisotropic displacement ellipsoids.

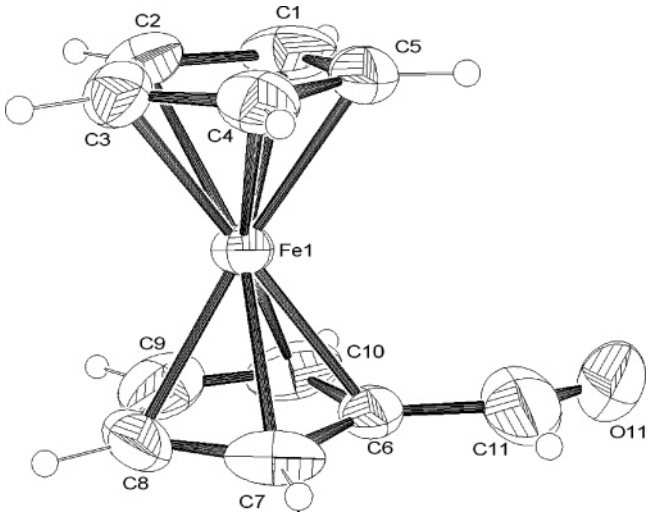

Figure 2. Molecular structure and atomic labeling scheme for ferrocenecarboxaldehyde with 50% anisotropic displacement ellipsoids.

Knudsen Effusion and Calvet-Drop Microcalorimetry Experiments. The vapor pressures, p, of ferrocene, 1,1′-dimethylferrocene, decamethylferrocene, and ferrocenecarboxaldehyde were studied as a function of the temperature by the Knudsen-effusion method. The values of p were calculated from[84,85]

$$p = \frac{m}{At}\left(\frac{2\pi RT}{M}\right)^{1/2}\left(\frac{8r+3l}{8r}\right)\left(\frac{2\lambda}{2\lambda+0.48r}\right) \quad (1)$$

where m is the mass loss during the time t; A, l, and r are the area, the thickness, and the radius of the effusion hole, respectively; M is the molar mass of the compound under study, R is the gas constant, T is the absolute temperature, and λ is the mean free path given by[86]

$$\lambda = \frac{kT}{\sqrt{2}\pi\sigma^2 p} \quad (2)$$

Here k represents the Boltzmann constant and σ the collision diameter. The collision diameters were estimated as 649 pm (ferrocene), 688 pm (1,1′-dimethylferrocene), 831 pm (decamethylferrocene), and 682 pm (ferrocenecarboxaldehyde) from the van der Waals volume of each molecule calculated with the GEPOL93 program,[87] using the van der Waals radii given by Bondi.[88] The vapor pressure against temperature data obtained (see Supporting Information) were fitted to[89]

$$\ln p = a + \frac{b}{T} \quad (3)$$

where the slope b is related to the enthalpy of sublimation at the average of the highest and lowest temperatures of the range covered in each series of experiments, T_m, by $\Delta_{sub}H^\circ_m(T_m) = -bR$. The experiments led to the a, b, and $\Delta_{sub}H^\circ_m(T_m)$ values indicated in Table 4, where the uncertainties quoted are the standard deviations of the mean multiplied by Student's factor for 95% confidence level.

The enthalpies of sublimation of ferrocene, 1,1′-dimethylferrocene, ferrocenecarboxaldehyde, α-methylferrocenemethanol and the enthalpy of vaporization of *N*,*N*-dimethyl(aminomethyl)-ferrocene, were also determined by Calvet-drop microcalorimetry at different reference temperatures, T_m. The results obtained are shown in Table 4 where the indicated uncertainties represent twice the standard deviation of the mean of five experiments in the case of 1,1′-dimethylferrocene and six experiments for the remaining compounds.

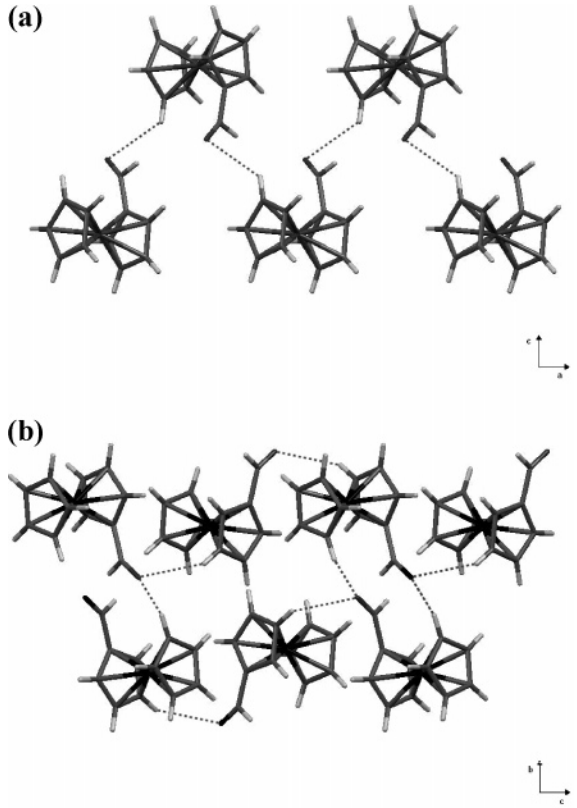

Figure 3. Crystal packing of ferrocenecarboxaldehyde showing (a) the formation of chains along the *a*-axis through hydrogen-bonding involving the aldehyde groups of two different molecules and (b) the formation of chains along the *b*-axis through a bifurcated hydrogen bond of the oxygen of the aldehyde substituent.

The values of $\Delta_{sub}H^{\circ}_{m}$ (T_m) in Table 4 were corrected to 298.15 K by using

$$\Delta_{sub}H^{\circ}_{m}(298.15\text{K}) = \Delta_{sub}H^{\circ}_{m}(T_m) + \int_{T_m}^{298.15\text{K}} [C^{\circ}_{p,m}(\text{g}) - C^{\circ}_{p,m}(\text{cr})]\, dT \quad (4)$$

where $C^{\circ}_{p,m}$(cr) and $C^{\circ}_{p,m}$(g) are the molar heat capacities of the compounds in the crystalline and gaseous states, respectively. An analogous equation was applied to the correction of $\Delta_{vap}H^{\circ}_{m}(T_m)$ in the case of *N*,*N*-dimethyl(aminomethyl)ferrocene. The obtained $\Delta_{vap}H^{\circ}_{m}$(298.15 K) and $\Delta_{sub}H^{\circ}_{m}$(298.15K) values are listed in Table 4. The heat capacities of the various compounds in different physical states were given as zero to second order polynomial equations:

$$C^{\circ}_{p,m} = a + bT + cT^2 \quad (5)$$

with T in K and $C^{\circ}_{p,m}$ in J·mol^{-1}·K^{-1}. The values of the *a*, *b* and *c* parameters used in the calculations are indicated in Table 5. For ferrocene these were obtained by fitting the heat capacity data reported for the solid[90−92] and gaseous compound[61,93] in the ranges 250−395 K and 298−700 K, respectively. In the case of 1,1′-dimethylferrocene the $C^{\circ}_{p,m}$ vs T equation was derived from a least-squares fitting of the heat capacity data determined in this work by DSC in the range 290−306 K. The heat capacity of the gas was estimated by assuming that $C^{\circ}_{p,m}(C_{12}H_{14}Fe,g) = C^{\circ}_{p,m}(C_{10}H_{10}Fe,g) + 2[C^{\circ}_{p,m}(C_6H_5CH_3,g) - C^{\circ}_{p,m}(C_6H_6,g)]$. The values of $C^{\circ}_{p,m}(C_{10}H_{10}Fe,g)$ were calculated from the data in Table 5, and those of $C^{\circ}_{p,m}(C_6H_5CH_3,g)$ and $C^{\circ}_{p,m}(C_6H_6,g)$ were taken from the literature.[94] The equations giving the heat capacities of solid and gaseous decamethylferrocene as a function of the temperature were previously reported.[61] In the case of solid ferrocenecarboxaldehyde the values in Table 5 were obtained by least-squares fitting of the heat capacity data published by Kaneko and Sorai in the range 296−313 K.[46] The corresponding parameters for the gas phase were derived from a least-squares fit of the heat capacity values in the range 200−400 K, calculated from statistical thermodynamics[95] using structural and vibration frequency data obtained at the B3PW91/SDDAll level of theory together with harmonic-oscillator/rigid-rotor partition functions. This theoretical approach was also used to obtain the data in Table 5 for gaseous α-methylferrocenemethanol. In this case, the average heat capacity of the solid obtained by Calvet microcalorimetry in the range 303−318 K was used. The heat capacities of liquid and gaseous *N*,*N*-dimethyl(aminomethyl)ferrocene were assumed to be constant between 298.15 and 305.1 K. The value of $C^{\circ}_{p,m}$(l) at 298.15 K given by Karyakin et al.[49] and the corresponding $C^{\circ}_{p,m}$(g) obtained at the B3PW91/SDDAll level of theory were used in eq 4 (Table 5).

Table 4 shows that the Knudsen effusion and Calvet-drop microcalorimetry experiments carried out for a given compound lead to $\Delta_{sub}H^{\circ}_{m}$(298.15K) results that are in good agreement within their combined uncertainty intervals. The enthalpy of sublimation of ferrocene has been determined in many laboratories and by a variety of techniques. The published data have been reviewed,[61,74] and a value of 73.48 ± 1.08 kJ·mol^{-1} has been proposed as reference.[74] This value is in good agreement with the results in Table 4, which refer to a sample analyzed for phase purity using X-ray powder diffraction.

To our knowledge the enthalpies of sublimation of 1,1′-dimethylferrocene and α-methylferrocenemethanol had not been reported.

The $\Delta_{sub}H^{\circ}_{m}$(298.15K) value for decamethylferrocene obtained in this work by the Knudsen effusion method is in good agreement with the Calvet-drop microcalorimetry result previously measured in our laboratory,[61] which is also included in Table 5 for comparison purposes.

The Knudsen effusion method has been applied by Karyakin et al.[49] to obtain the vapor pressures of solid ferrocenecarboxaldehyde and liquid *N*,*N*-dimethyl(aminomethyl)ferrocene as a function of the temperature in the ranges 323.75−343.55 K and 295.45−318.75 K, respectively. From a least-squares fit to their data it is possible to derive the following parameters of eq 3: $a = 24.47 \pm 3.52$, $b = -8186.6 \pm 1177.8$ for ferrocenecarboxaldehyde, and $a = 24.58 \pm 4.08$ and $b = -7864.6 \pm 1254.5$ for *N*,*N*-dimethyl(aminomethyl)ferrocene. The indicated uncertainties include Student's factor for 95% confidence level: $t = 2.571$ for Fe[(η^5-C_5H_5)(η^5-C_5H_4CHO)] (6 data points) and $t = 2.776$ for Fe[(η^5-C_5H_5){η^5-$C_5H_4CH_2N(CH_3)_2$}] (5 data points). Hence $\Delta_{sub}H^{\circ}_{m}$ {Fe[(η^5-C_5H_5)(η^5-C_5H_4CHO)], 333.7 K} = 68.1 ± 9.8 kJ·mol^{-1} and $\Delta_{vap}H^{\circ}_{m}$ Fe[(η^5-C_5H_5){η^5-$C_5H_4CH_2N(CH_3)_2$}], 307.1 K} = 65.4 ± 10.4 kJ·mol^{-1} are obtained. These values lead to $\Delta_{sub}H^{\circ}_{m}$ {Fe[(η^5-C_5H_5)(η^5-C_5H_4CHO)], 298.15 K} = 70.4 ± 9.8 kJ·mol^{-1} and $\Delta_{vap}H^{\circ}_{m}$ Fe[(η^5-C_5H_5){η^5-$C_5H_4CH_2N(CH_3)_2$}], 298.15 K} = 66.4 ± 10.4 kJ·mol^{-1}, after the appropriate corrections using the heat capacity data in Table 5 are applied. While the latter value agrees with the corresponding result in Table 4 within their combined uncertainties, the former shows a significant discrepancy despite its large uncertainty. This discrepancy is mainly due to the fact that our experiments and those of Karyakin et al.[49] were carried in temperature ranges where ferrocenecarboxaldehyde exists as different solid phases. The compound exhibits a phase transition from a crystalline phase (Phase II) to a plastic crystalline phase

TABLE 4: Parameters of Eq 3 and Enthalpies of Sublimation and Vaporization (Data in kJ·mol^{-1})

compound	method	a	$-b$	T_m/K	$\Delta_{sub}H^\circ_m(T_m)$ or $\Delta_{vap}H^\circ_m(T_m)$	$\Delta_{sub}H^\circ_m$(298.5K) or $\Delta_{vap}H^\circ_m$(298.5K)
Fe(η^5-C_5H_5)$_2$, cr	Knudsen[a]	29.39 ± 0.78	8797.6 ± 234.8	300.8	73.15 ± 1.95	73.28 ± 1.95
	Calvet			298.15		72.71 ± 0.23
Fe(η^5-$C_5H_4CH_3$)$_2$, cr	Knudsen[b]	36.49 ± 0.80	10460.6 ± 227.3	280.2	86.97 ± 1.89	84.51 ± 1.89
	Calvet			298.15		84.72 ± 0.22
Fe[η^5-$C_5(CH_3)_5$]$_2$, cr	Knudsen[c]	31.22 ± 0.78	11509.8 ± 285.5	364.7	95.70 ± 2.37	98.98 ± 2.37
	Calvet			362.0[e]	93.69 ± 0.55[e]	96.81 ± 0.55[e]
Fe[(η^5-C_5H_5)(η^5-C_5H_4CHO)], cr	Knudsen[d]	33.31 ± 2.01	10749.4 ± 610.6	304.5	89.38 ± 5.08	89.72 ± 5.08
	Knudsen[d]	32.50 ± 1.36	10490.9 ± 425.3	310.1	87.23 ± 3.54	87.90 ± 3.54
	Calvet			311.2	87.81 ± 0.49	88.54 ± 0.49
Fe[(η^5-C_5H_5)(η^5-$C_5H_4CHCH_3OH$)], cr	Calvet			311.0	102.03 ± 0.90	102.35 ± 0.90
Fe[(η^5-C_5H_5){η^5-$C_5H_4CH_2N(CH_3)_2$}],1	Calvet			305.1	73.01 ± 0.40	73.80 ± 0.40

[a] Hole 1 ($A = 6.952 \times 10^{-7}$ m^2, $l = 2.090 \times 10^{-5}$ m, $r = 4.704 \times 10^{-4}$ m), $\sigma = 649$ pm. [b] Hole 2 ($A = 4.390 \times 10^{-7}$ m^2, $l = 2.090 \times 10^{-5}$ m, $r = 3.738 \times 10^{-4}$ m), $\sigma = 688$ pm. [c] Hole 2 ($A = 4.390 \times 10^{-7}$ m^2, $l = 2.090 \times 10^{-5}$ m, $r = 3.738 \times 10^{-4}$ m), $\sigma = 831$ pm. [d] Hole 3 ($A = 6.910 \times 10^{-7}$ m^2, $l = 2.090 \times 10^{-5}$ m, $r = 4.690 \times 10^{-4}$ m), $\sigma = 682$ pm. [e] Reference 61.

TABLE 5: Values of the *a*, *b*, and *c* Parameters in Eq 5

compound	state	a	b	$c \times 10^4$
Fe(η^5-C_5H_5)$_2$	cr	−68.063	1.0622	−6.1555
	g	−56.999	0.7955	−3.7825
Fe(η^5-$C_5H_4CH_3$)$_2$	cr	−182.28	1.7467	
	g	−13.138	0.6887	
Fe[η^5-$C_5(CH_3)_5$]$_2$	cr[a]	1066.6	−4.2591	75.951
	g[a]	180.24	1.0418	−7.5097
Fe[(η^5-C_5H_5)	cr	−193.90	1.4571	
(η^5-C_5H_4CHO)]	g	1.4768	0.6410	
Fe[(η^5-C_5H_5)	cr	259.7		
(η^5-$C_5H_4CHCH_3OH$)]	g	6.9778	0.7463	
Fe[(η^5-C_5H_5)	l	363.0		
{η^5-$C_5H_4CH_2N(CH_3)_2$}]	g	249.8		

[a] Reference 61.

(Phase I) at 316.7 K, with $\Delta_{trs}H^\circ_m$(II→I) = 11.7 ± 0.3 kJ·mol^{-1}.[46] This value fully accounts for the difference between the $\Delta_{sub}H^\circ_m$ results obtained by us and by Karyakin et al.,[49] when their combined uncertainties are considered.

Molecular Dynamics (MD) Simulations. The simulation results are compared in Table 6 with the corresponding experimental data taken from the literature or obtained in this work from X-ray diffraction, Knudsen effusion or Calvet microcalorimetry experiments.

For ferrocene, 1,1′-dimethylferrocene, ferrocenecarboxaldehyde, α-methylferrocenemethanol, and *N*,*N*-dimethyl(aminomethyl)ferrocene, the calculated and experimental densities exhibit deviations, $\delta\rho$, smaller than 3%. These deviations are similar to those obtained by other authors when comparing the performance of a given force field against experimental density data for molecular compounds, in both the liquid and crystalline phases.[70,71] The agreement between the experimental ρ values and those obtained in this work from MD simulations is very good, considering that the calculations are purely predictive: all structure-dependent parameters used were either directly taken from the OPLS-AA force field or obtained from DFT calculations; none was adjusted to match experimental crystallographic data. The model was also able to accurately predict the structural properties of the solid compounds ferrocene, 1,1′-dimethylferrocene, ferrocenecarboxaldehyde, and α-methylferrocenemethanol. In general, after relaxation, the experimental unit cell dimensions and angles were reproduced with deviations of less than 1%. It must be noted that all MD data presented in Table 6 (cell parameters and volume of the cell) were obtained by direct averaging of the simulation results. Any apparent inconsistency between the values of the cell parameters and the cell volumes in that table is, therefore, due to this fact.

As mentioned above, the nonbonded interaction parameter, ϵ, for iron was adjusted so that the simulations could reproduce the experimental value of the standard molar enthalpy of sublimation of ferrocene (73.0 ± 0.3 kJ·mol^{-1}, this work). After this adjustment the model was able to predict the standard molar enthalpies of sublimation of 1,1′-dimethylferrocene, ferrocenecarboxaldehyde, and α-methylferrocenemethanol, and the value of $\Delta_{vap}H^\circ_m$(298.5K) of *N*,*N*-dimethyl(aminomethyl)ferrocene, within their combined uncertainties, the maximum absolute deviations being smaller than 5 kJ·mol^{-1} and the corresponding relative errors varying in the range 2%−6%. Relative errors larger than those observed for the structural parameters are to be expected in this case. In fact, the standard molar enthalpies of sublimation or vaporization are calculated as

$$\Delta_{sub}H^\circ_m = U^\circ_{conf,m}(g) - U^\circ_{conf,m}(cr) + RT \quad (6)$$

$$\Delta_{vap}H^\circ_m = U^\circ_{conf,m}(g) - U^\circ_{conf,m}(l) + RT \quad (7)$$

where $U^\circ_{conf,m}$ represents the standard molar configurational internal energy. Thus, unlike the density and other structural parameters, which are obtained from a single simulation run modeling the condensed phase (crystalline or liquid), the calculation of $\Delta_{sub}H^\circ_m$ or $\Delta_{vap}H^\circ_m$ involves the difference between two configurational internal energy values, $U^\circ_{conf,m}(g) - U^\circ_{conf,m}(cr)$ or $U^\circ_{conf,m}(g) - U^\circ_{conf,m}(l)$. These are obtained from two independent simulation runs, one referring to the condensed phase and another to the gas phase. The uncertainties associated with each run will add up in the calculation of the errors of the differences in eqs 6 and 7. Thus, when both $U^\circ_{conf,m}$ contributions are large and have the same sign, their difference is smaller than each of the individual values and a large relative error can occur. This is especially relevant in the case of simulations performed in the gas phase with a single molecule. Although the simulation times are generally extended over very large periods of time (typically 2 orders of magnitude larger than in the corresponding condensed-phase simulation runs), the fluctuations associated with any given configuration lead to values with large uncertainty intervals.

It is apparent from Table 6 that for decamethylferrocene the observed deviations between the predicted and experimental values of the structural and energetic properties are considerably larger than for the other compounds studied in this work. The origin of the poorer performance of the model in this case warrants a more detailed analysis. The interactions that contribute to the molar internal energy of a given configuration are normally subdivided into two groups: (i) the nonbonded interactions, which include van der Waals and Coulombic interactions, and (ii) the bonded interactions comprising bond, angle, and dihedral interactions. Although the former group is generally associated with intermolecular interactions (those that

TABLE 6: Comparison of the Simulation Results with the Corresponding Structural and Energetic Data, Experimentally Obtained from X-ray Diffraction or Enthalpy of Sublimation Measurements

compound		Fe (η^5-C_5H_5)$_2$, cr	Fe (η^5-$C_5H_4CH_3$)$_2$, cr	Fe [η^5-$C_5(CH_3)_5$]$_2$, cr	Fe[(η^5-C_5H_5)(η^5-$C_5H_4CHCH_3OH$)], cr	Fe[(η^5-C_5H_5)(η^5-C_5H_4CHO)], cr	Fe[(η^5-C_5H_5){(η^5-$C_5H_4CH_2N(CH_3)_2$}], 1
				Simulation Details			
molecules		280	240	144	256	144	200
unit cells/simulation		4 × 5 × 7	3 × 5 × 4	3 × 3 × 4	2 × 2 × 4	4 × 3 × 3	1 × 1 × 1
				Simulation Results (MD) and Experimental Crystallographic data (XRD) at 298 K			
a/Å	MD	10.63 ± 0.07	11.0 ± 0.1	14.6 ± 0.2	23.2 ± 0.1	7.61 ± 0.04	
	XRD	10.530[a]	10.954[b]	15.210[c]	23.3334[d]	7.639[e]	
b/Å	MD	7.65 ± 0.03	7.51 ± 0.07	12.3 ± 0.1	23.2 ± 0.1	10.3 ± 0.1	
	XRD	7.604[a]	7.526[b]	11.887[c]	23.3334[d]	10.525[e]	
c/Å	MD	5.93 ± 0.04	12.21 ± 0.07	9.7 ± 0.2	8.01 ± 0.03	12.0 ± 0.1	
	XRD	5.925[a]	12.334[b]	9.968[c]	7.7186[d]	11.294[e]	
α/deg	MD	90.0 ± 0.1	90.0 ± 0.1	90.0 ± 0.1	90.0 ± 0.1	90.0 ± 0.1	
	XRD	90[a]	90[b]	90[c]	90[d]	90[e]	
β/deg	MD	121.6 ± 0.1	102.0 ± 0.2	86 ± 2	90.0 ± 0.1	90.0 ± 0.1	
	XRD	121.05[a]	102.81[b]	90[c]	90[d]	90[e]	
γ/deg	MD	89.9 ± 0.1	90.1 ± 0.2	90.0 ± 0.1	90.1 ± 0.2	90.0 ± 0.1	
	XRD	90[a]	90[b]	90[c]	90[d]	90[e]	
V_{cell}/Å^3	MD	409 ± 3	1000 ± 6	1707 ± 30	4294 ± 27	938 ± 6	
	XRD	406	992	1802	4202	908	
ρ/g·cm^{-3}	MD	**1.51 ± 0.01**	**1.42 ± 0.01**	**1.27 ± 0.02**	**1.42 ± 0.01**	**1.52 ± 0.01**	**1.25 ± 0.01**
	XRD	1.520	1.434	1.203	1.455	1.566	1.228[f]
$\delta\rho$/%		−0.8	−0.9	5.6	−2.4	−2.9	1.8
				Simulation (MD) Results and Experimental Values (Exp) of the Enthalpies of Sublimation at 298 K			
$U_{c,m}$(cr or l)/kJ·mol^{-1}	MD	−28.8 ± 0.6	−45.0 ± 1.3	−152.7 ± 1.4	−83.4 ± 0.6	−19.4 ± 3.4	75.5 ± 1.2
$U_{c,m}$(gas)/kJ·mol^{-1}	MD	42.3 ± 3	34 ± 4	−41 ± 4	20 ± 3	68 ± 3	151 ± 5
$\Delta_{sub\ or\ vap}U_{c,m}$/kJ·mol^{-1}	MD	71 ± 4	79 ± 5	112 ± 5	103 ± 4	87 ± 6	76 ± 6
$\Delta_{sub\ or\ vap}H^\circ_m$/kJ·mol^{-1}							
	MD	**73 ± 4**	**81 ± 5**	**114 ± 5**	**105 ± 4**	**90 ± 6**	**78 ± 6**
	Exp	73.0 ± 0.3[g]	84.6 ± 0.1[g]	97.9 ± 1.1[g]	102.4 ± 0.9[h]	88.7 ± 0.7[g]	73.8 ± 0.4[i]
$\delta\ \Delta_{sub\ or\ vap}H^\circ_m$/kJ·mol^{-1}		0.0[j]	−3.6	16.1	2.6	1.3	4.2

[a] Reference 36. [b] This work. [c] Reference 43. [d] Reference 48. [e] Reference 44. [f] Density in the liquid state. [g] Mean of the enthalpy of sublimation values at 298.15 K obtained by the Knudsen effusion and Calvet microcalorimetry methods and reported in Table 4; the uncertainty quoted is the mean deviation of the results. [h] Enthalpy of sublimation at 298.15 K obtained by Calvet microcalorimetry and indicated in Table 4. [i] Enthalpy of vaporization at 298.15 K obtained by Calvet microcalorimetry and reported in Table 4. [j] The ϵ parameter for iron was selected so that the enthalpy of sublimation of ferrocene predicted by the MD simulations matched the experimental value.

need to be considered when dealing with vaporization or sublimation processes) and the latter group with intramolecular interactions (whose contribution to a vaporization or sublimation process generally cancels out), the separation line is not well-defined, since there are also nonbonded interactions that act at the intramolecular level. Within the OPLS-AA framework any two atoms of the same molecule separated by three bonds will interact *via* nonbonded interactions with 50% intensity and those further apart with full-intensity nonbonded interactions.

When the different bonded and nonbonded contributions to $U^\circ_{conf,m}$(g), $U^\circ_{conf,m}$(cr) or $U^\circ_{conf,m}$(l) are computed for ferrocene and all ferrocene derivatives studied in this work, except for decamethylferrocene, the contributions from the bonded interactions are almost identical in the gas and condensed phases and cancel out in the calculation of $\Delta_{sub}H^\circ_m$ or $\Delta_{vap}H^\circ_m$ through eqs (6) and (7), respectively. That is not the case for decamethylferrocene, where the value of $\Delta_{sub}U^\circ_m = U^\circ_{conf,m}(g) - U^\circ_{conf,m}$(cr) can be expressed as a sum of nonbonded and bonded contributions: $\Delta_{sub}U^\circ_m = 112$ kJ·mol^{-1} = $\Delta_{sub}U^\circ_m$(nonbonded-interactions) + $\Delta_{sub}U^\circ_m$(bonded-interactions) = (106 + 6) kJ·mol^{-1}. If the bonded contribution is not taken into account in the calculation of $\Delta_{sub}H^\circ_m$ (since intramolecular interactions that are both present in the gas and solid phases should not contribute significantly to the sublimation process), a value $\Delta_{sub}H^\circ_m$ {Fe[η^5-$C_5(CH_3)_5$]$_2$, 298.15 K} = 108 kJ·mol^{-1} is obtained, which compares more favorably than 114 ± 5 kJ·mol^{-1} with the experimental value 97.9 ± 1.1 kJ·mol^{-1} measured in this work in (Table 6). The agreement between the simulated and experimental values could be improved if it was possible to calculate the contribution from nonbonded interactions that are acting at an intramolecular level and (like their bonded counterparts) do not cancel between the gaseous and condensed phases. If we assume that such a contribution is similar to that from the bonded interactions (6 kJ·mol^{-1}), the $\Delta_{sub}H^\circ_m$ {Fe[η^5-$C_5(CH_3)_5$]$_2$, 298.15 K} value estimated from the simulation data would further decrease to 102 ± 5 kJ·mol^{-1}, thus becoming in agreement with the experimental results, within their combined uncertainty intervals.

Although we can explain the overestimation of $\Delta_{sub}H^\circ_m$ in the case of decamethylferrocene in a phenomenological way (the noncancellation of the intramolecular interactions in the gas and condensed phase), two issues remain to be addressed: the inability of the model to avoid such an error and the physical causes (at a molecular level) that lead to its manifestation.

The rotation of the methyl substituents in decamethylferrocene is extremely hindered[31] and requires some degree of coordinated movement between the different groups. This means that nonbonded interactions between atoms belonging to those groups (for instance between a given hydrogen atom and the carbon atom of an adjacent methyl group or between two hydrogen atoms belonging to two adjacent methyl groups) take place at shorter distances than nonbonded interactions between methyl groups belonging to different molecules (or even belonging to the same molecule but unhindered). In other words the parametrization of methyl (or any other) groups within the OPLS-AA force field is ill-suited to model molecules with such type of extreme hindrance. However, even if the model is unsuitable to describe decamethylferrocene and similar molecules, probably overestimating the magnitude of the attractive interactions in both the gas and condensed phases (note the

negative value $U^{\circ}_{conf,m}(g) = -41 \pm 4$ kJ·mol^{-1}, in Table 6 which contrasts with the corresponding positive values for the other ferrocene derivatives), it could still yield accurate $\Delta_{sub}H^{\circ}_{m}$ results if the (wrong) configurational energy contributions of the gaseous and condensed phases canceled out. That is not the case, simply because at the molecular level the hindered rotation of the methyl groups (and the corresponding coordinated movements) is probably much different for an isolated molecule in the gas phase than for a molecule surrounded by similar neighbors in the condensed phase.

The failure of the model to predict the properties of decamethylferrocene can in fact be viewed as an asset: it clearly demonstrates that one should be careful when attempting to apply the present model (or its underlying OPLS-AA framework) to the modeling of very hindered molecules; it also stresses the issue of the model autoconsistency: whenever the model yields inaccurate energetic properties the impact on the structural properties is also evident.

In conclusion, the results obtained indicate that the present model can be regarded as another step toward a general and simple force field for metallocenes, built in a coherent way, easily integrated with the OPLS-AA force field, and transferable within significantly different members of the ferrocene family. The extension of this proposed DFT/MD methodology to metallocenes of other transition metals, in conjunction with accurate enthalpy of sublimation measurements for validation of the corresponding energy-dependent parametrization, is currently in progress.

Acknowledgment. This work was supported by Fundação para a Ciência e a Tecnologia, Portugal (Project POCTI/199/QUI/35406). A Ph.D. grant from FCT is gratefully acknowledged by S.S.P. (SFRH/BD/12330/2003).

Supporting Information Available: Figures S1−S5 with the powder diffractograms and Tables S1−S5 with the indexation of the powder diffraction lines for the solid compounds studied in this work. The CIF files with the crystallographic parameters and structural data of dimethylferrocene at 293 K and of ferrocenecarboxaldehyde at 150 K. Table S6 with the vapor pressure against temperature data for all compounds studied by the Knudsen effusion method. This material is available free of charge via the Internet at http://pubs.acs.org.

References and Notes

(1) *Bonding Energetics in Organometallic Compounds*; Marks, T. J., Ed.; American Chemical Society: Washington, 1990.
(2) *Energetics of Organometallic Species*; Martinho Simões, J. A., Ed.; Kluwer: Dordrecht, 1992.
(3) Martinho Simões, J. A.; Minas da Piedade, M. E. Structure and Bonding in Organometallic Compounds: Organometallic Thermochemistry. In *Comprehensive Organometallic Chemistry III*; Parkin, G., Ed.; Elsevier: Oxford, 2007; Vol. 1, Fundamentals, p 605.
(4) *The Chemistry of Metal CVD*; Hampden-Smith, T. T., Kodas, M. J., Eds.; John Wiley: New York, 1994.
(5) *Handbook of Chemical Vapour Deposition (CVD)*, 2nd ed.; Noyes Pub.: NJ, 1999.
(6) Bondi, A. *J. Chem. Eng. Data* **1963**, *8*, 381.
(7) Wakayama, N.; Inokuchi, H. *Bull. Chem. Soc. Jpn.* **1967**, *40*, 2267.
(8) Davies, M. *J. Chem. Educ.* **1971**, *48*, 591.
(9) Morawetz, E. *J. Chem. Thermodyn.* **1972**, *4*, 461−467.
(10) Nass, K.; Lenoir, D.; Kettrup, A. *Angew. Chem., Int. Ed. Engl.* **1995**, *34*, 1735.
(11) Chickos, J. S.; Hesse, D. G.; Liebman, J. F. Estimating Enthalpies of Sublimation of Hydrocarbons. In *Energetics of Organometallic Species*; Martinho Simões, J. A., Ed.; Kluwer: Dordrecht, 1992; p 159.
(12) Chickos, J. S.; Acree, W. E., Jr.; Liebman, J. F. Estimating Enthalpies of Sublimation of Hydrocarbons. In *Computational Thermochemistry*; Irikura, K. K., Frurip, D. J., Eds.; American Chemical Society: Washington, 1998; p 63.
(13) Chearlton, M. H.; Docherty, R.; Hutchings, M. G. *J. Chem. Soc., Perkin Trans. 2* **1995**, 2023.
(14) Westwell, M. S.; Searle, M. S.; Wales, D. J.; Williams, D. *J. Am. Chem. Soc.* **1995**, *117*, 5013.
(15) Gavezzotti, A. *Acc. Chem. Res.* **1994**, *27*, 309.
(16) Rabinovich, I. B.; Nistratov, V. P.; Tel'noi, V. I.; Sheiman, M. S. *Thermochemical and Thermodynamic Properties of Organometallic Compounds*; Begell House: New York, 1999.
(17) Chickos, J. S.; Acree, W. E., Jr. *J. Phys. Chem. Ref. Data* **2002**, *31*, 537.
(18) Martinho Simões, J. A. Organometallic Thermochemistry Data. In *NIST Chemistry WebBook; NIST Standard Reference Database Number 69*; Linstrom, P. J., Mallard, W. G., Eds.; National Institute of Standards and Technology: Gaithersburg, 2005.
(19) Diogo, H. P.; Minas da Piedade, M. E.; Gonçalves, J. M.; Monte, M. J. S.; Ribeiro da Silva, M. A. V. *Eur. J. Inorg. Chem.* **2001**, *228*, 257.
(20) Pertsin, A. J.; Kitaigorodsky, A. I. *The Atom-Atom Potential Method. Applications to Organic Molecular Solids*; Springer-Verlag: Berlin, 1987.
(21) *Theoretical Aspects and Computer Modelling of the Molecular Solid State*; Gavezzotti, A., Ed.; John Wiley: Chichester, 1997.
(22) Lommerse, J. P. M.; Motherwell, W. D. S.; Ammon, H. L.; Dunitz, J. D.; Gavezzotti, A.; Hofmann, D. W. M.; Leusen, F. J. J.; Mooji, W. T. M.; Price, S. L.; Schweizer, B.; Schmidt, M. U.; van Eijck, B. P.; Verwer, P.; Williams, D. E. *Acta Crystallogr.* **2000**, *B56*, 697.
(23) Motherwell, W. D. S.; Ammon, H. L.; Dunitz, J. D.; Dzyabchenko, A.; Erk, P.; Gavezzotti, A.; Hofmann, D. W. M.; Leusen, F. J. J.; Lommerse, J. P. M.; Mooij, W. T. M.; Price, S. L.; Scheraga, H.; Schweizer, B.; Schmidt, M. U.; van Eijck, B. P.; Verwer, P.; Williams, D. E. *Acta Crystallogr.* **2002**, *B58*, 647.
(24) Day, G. M.; Motherwell, W. D. S.; Ammon, H. L.; Boerrigter, S. X. M.; Della, Valle, R. G.; Venuti, E.; Dzyabchenko, A.; Dunitz, J. D.; Schweizer, B.; van Eijck, B. P.; Erk, P.; Facelli, J. C.; Bazterra, V. E.; Ferraro, M. B.; Hofmann, D. W. M.; Leusen, F. J. J.; Liang, C.; Pantelides, C. C.; Karamertzanis, P. G.; Price, S. L.; Lewis, T. C.; Nowell, H.; Torrisi, A.; Scheraga, H. A.; Arnautova, Y. A.; Schmidt, M. U.; Verwer, P. *Acta Crystallogr.* **2005**, *B61*, 511.
(25) *Crystal Engineering: From Molecules and Crystals to Materials*; Braga, D., Grepioni, F., Orpen, A. G., Eds.; Kluwer: Dordrecht, 1999.
(26) Welsh, W. J.; Tong, W.; Collantes, E. R.; Chickos, J. S.; Gagarin, S. G. *Thermochim. Acta* **1996**, *290*, 55.
(27) Puri, S.; Chickos, J. S.; Welsh, W. J. *J. Chem. Inf. Comput. Sci.* **2002**, *42*, 109.
(28) Gavezzotti, A. *Z. Kristallogr.* **2005**, *220*, 499.
(29) Gavezzotti, A. *Synlett* **2002**, *B56* 201.
(30) Allen, F. H. *Acta Crystallogr.* **2002**, *B58*, 380.
(31) Canongia Lopes, J. N.; Cabral do Couto, P.; Minas da Piedade, M. E. *J. Phys. Chem. A* **2006**, *110*, 13850.
(32) Laugier, J.; Bochu, B. *Checkcell*. http://www.ccp14.ac.uk/tutorial/Imgp.
(33) Moura Ramos, J. J.; Taveira-Marques, R.; Diogo, H. P. *J. Pharm. Sci.* **2004**, *93*, 1503.
(34) Nakamoto, K. *Infrared and Raman Spectra of Inorganic and Coordination Compounds*, Part B, 5th ed.; Wiley: New York, 1997.
(35) Saito, T.; Hayamizu, K.; Yanagisawa, M.; Yamamoto, O.; Wasada, N.; Someno, K.; Kinugasa, S.; Tanabe, K.; Tamura, T.; Hiraishi, J. *Spectral Database for Organic Compounds, SDBS*; National Institute of Advanced Industrial Science and Technology (AIST): Japan, 2006.
(36) Takusagawa, T.; Koetzle, T. F. *Acta Crystallogr.* **1979**, *B35*, 1074.
(37) Joens, O.; Gjaldback, D. *Dan. Tidsskr. Farm.* **1969**, *43*, 151.
(38) Beech, G.; Lintonbon, R. M. *Thermochim. Acta* **1971**, *2*, 86.
(39) Murray, J. P.; Cavell, K. J.; Hill, J. O. *Thermochim. Acta* **1980**, *36*, 97.
(40) Phillips, L.; Lacey, A. R.; Cooper, M. K. *J. Chem. Soc., Dalton Trans.* **1988**, 1383.
(41) Kim, D.-H.; Ryu, E.-S.; Cho, C. S.; Shim, S. C.; Kim, H.-S.; Kim, T.-J. *Organometallics* **2000**, *19*, 5784.
(42) Stanghellini, P. L.; Diana, E.; Boccaleri, E.; Rossetti, R. *J. Organomet. Chem.* **2000**, *593*−*594*, 36.
(43) Freyberg, D. P.; Robbins, J. L.; Raymond, K. N.; Smart, J. C. *J. Am. Chem. Soc.* **1979**, *101*, 892.
(44) Sato, K.; Iwai, M.; Sano, H.; Konno, M. *Bull. Chem. Soc. Jpn.* **1984**, *57*, 634.
(45) Daniel, D. M.; Leadbetter, A. L.; Meads, R. E.; Parker, W. G. *J. Chem. Soc., Faraday Trans. 2* **1978**, *74*, 456.
(46) Kaneko, Y.; Sorai, M. *Phase Transitions* **2007**, *80*, 517−528.
(47) Rosol, M. *Synthesis and Study of New Cyclometallated Derivatives of Ferrocene*; Ph.D. Thesis; University of Barcelona, 2007.
(48) Glidewell, C.; Klar, R. B.; Lightfoot, P.; Zakaria, C. M.; Ferguson, G. *Acta Crystallogr.* **1996**, *B52*, 110.
(49) Karyakin, N. V.; Kozlova, M. S.; Sheiman, M. S.; Kamelova, G. P.; Larina, V. N. *Russ. J. Phys. Chem.* **2003**, *77*, 1230.
(50) Farrugia, L. J. *J. Appl. Crystallogr.* **1999**, *32*, 837−838.

(51) Harms, K.; Wocadlo, S. *XCAD4-CAD4 Data Reduction*; University of Marburg: Marburg, Germany, 1995.

(52) *SADABS; Area-Detector Absorption Correction*; Bruker AXS Inc.: Madison, 2004.

(53) *SAINT: Area-Detector Integration Software*, version 7.23; Bruker AXS Inc.: Madison, 2004.

(54) Altomare, A.; Burla, M. C.; Camalli, M.; Cascarano, G.; Giacovazzo, G.; Guagliardi, A.; Moliterini, A. G. G.; Polidoro, G.; Spagna, R. *J. Appl. Crystallogr.* **1999**, *32*, 115.

(55) Sheldrick, G. M. *SHELXL-97: Program for the Refinement of Crystal Structure*; University of Göttingen: Germany, 1997.

(56) Farrugia, L. J. *J. Appl. Crystallogr.* **1997**, *30*, 565.

(57) Macrae, C. F.; Edgington, P. R.; McCabe, P.; Pidcock, E.; Shields, G. P.; Taylor, R.; Towler, M.; van de Streek, J. *J. Appl. Crystallogr.* **2006**, *39*, 453.

(58) Nardelli, M. *J. Appl. Crystallogr.* **1995**, *28*, 659.

(59) Calado, J. C. G.; Dias, A. R.; Minas da Piedade, M. E.; Martinho Simões, J. A. *Rev. Port. Quim.* **1980**, *22*, 53.

(60) Diogo, H. P.; Minas da Piedade, M. E.; Fernandes, A. C.; Martinho Simões, J. A.; Ribeiro da Silva, M. A. V.; S., M. M. J. *Thermochim. Acta* **1993**, *228*, 15.

(61) Kiyobayashi, T.; Minas da Piedade, M. E. *J. Chem. Thermodyn.* **2001**, *33*, 11.

(62) Bernardes, C. E. S.; Santos, L. M. N. B. F.; Minas da Piedade, M. E. *Meas. Sci. Technol.* **2006**, *17*, 1405.

(63) Frisch, M. J.; Trucks, G. W.; Schlegel, H. B.; Scuseria, G. E.; Robb, M. A.; Cheeseman, J. R.; Montgomery, J. A., Jr.; Vreven, T.; Kudin, K. N.; Burant, J. C.; Millam, J. M.; Iyengar, S. S.; Tomasi, J.; Barone, V.; Mennucci, B.; Cossi, M.; Scalmani, G.; Rega, N.; Petersson, G. A.; Nakatsuji, H.; Hada, M.; Ehara, M.; Toyota, K.; Fukuda, R.; Hasegawa, J.; Ishida, M.; Nakajima, T.; Honda, Y.; Kitao, O.; Nakai, H.; Klene, M.; Li, X.; Knox, J. E.; Hratchian, H. P.; Cross, J. B.; Bakken, V.; Adamo, C.; Jaramillo, J.; Gomperts, R.; Stratmann, R. E.; Yazyev, O.; Austin, A. J.; Cammi, R.; Pomelli, C.; Ochterski, J. W.; Ayala, P. Y.; Morokuma, K.; Voth, G. A.; Salvador, P.; Dannenberg, J. J.; Zakrzewski, V. G.; Dapprich, S.; Daniels, A. D.; Strain, M. C.; Farkas, O.; Malick, D. K.; Rabuck, A. D.; Raghavachari, K.; Foresman, J. B.; Ortiz, J. V.; Cui, Q.; Baboul, A. G.; Clifford, S.; Cioslowski, J.; Stefanov, B. B.; Liu, G.; Liashenko, A.; Piskorz, P.; Komaromi, I.; Martin, R. L.; Fox, D. J.; Keith, T.; Al-Laham, M. A.; Peng, C. Y.; Nanayakkara, A.; Challacombe, M.; Gill, P. M. W.; Johnson, B.; Chen, W.; Wong, M. W.; Gonzalez, C.; Pople, J. A. *Gaussian 03*, revision C.02; Gaussian, Inc.: Wallingford, 2004.

(64) Becke, A. D. *J. Chem. Phys.* **1993**, *98*, 5648.

(65) Perdew, J. P.; Wang, Y. *Phys. Rev. B* **1992**, *45*, 13244.

(66) Leininger, T.; Nicklass, A.; Stoll, H.; Dolg, M.; Schwerdtfeger, P. *J. Chem. Phys.* **1996**, *105*, 1052.

(67) Dunning, T. H., Jr.; Hay, P. J. *Modern Theoretical Chemistry*; Schaefer, H. F., III, Ed.; Plenum: New York, 1976; Vol. 3; p 1.

(68) Breneman, C. M.; Wiberg, K. B. *J. Comput. Chem.* **1990**, *11*, 361.

(69) Smith, W.; Forester, T. R. *The DL_POLY Package of Molecular Simulation Routines*, v. 2.12; The Council for The Central Laboratory of Research Councils; Daresbury Laboratory: Warrington, 1999.

(70) Jorgensen, W. L.; Maxwell, D. S.; Tirado-Rives, J. *J. Am. Chem. Soc.* **1996**, *118*, 11225.

(71) Kaminski, G.; Jorgensen, W. L. *J. Phys. Chem.* **1996**, *100*, 18010.

(72) Cornell, W. D.; Cieplak, P.; Bayly, C. I.; Gould, I. R.; Merz, K. M.; Ferguson, D. M.; Spellmeyer, D. C.; Fox, T.; Caldwell, J. W.; Kollman, P. A. *J. Am. Chem. Soc.* **1995**, *117*, 5179.

(73) Parameters obtained from file parm99.dat corresponding to AMBER versions 1999 and 2002.

(74) *Reference Materials for Calorimetry and Differential Thermal Analysis*; Sabbah, R., Ed.; *Thermochim. Acta* **1999**, *331*, 93.

(75) Gavezzotti, A.; Filippini, G. Energetic Aspects of Crystal Packing: Experimental and Computer Simulations. In *Theoretical Aspects and Computer Modelling of the Molecular Solid State*; Gavezzotti, A., Ed.; John Wiley: Chichester, 1997; p 67.

(76) Seiler, P.; Dunitz, J. D. *Acta Crystallogr.* **1979**, *B35*, 1068.

(77) Seiler, P.; Dunitz, J. D. *Acta Crystallogr.* **1982**, *B38*, 1741.

(78) Brock, C. P.; Yigang, F. *Acta Crystallogr.* **1997**, *B52*, 928.

(79) Foucher, D. A.; Honeyman, C. H.; Lough, A. J.; Manners, I.; Nelson, J. M. *Acta Crystallogr.* **1995**, *C51*, 1795.

(80) Santos, L. M. N. B. F.; Canongia, Lopes, J. N.; Coutinho, J. A. P.; Esperança, J. M. S. S.; Gomes, L. R.; Marrucho, I. M.; Rebelo, L. P. N. *J. Am. Chem. Soc.* **2007**, *129*, 284.

(81) Wieser, M. E. *Pure Appl. Chem.* **2006**, *78*, 2051.

(82) Seiler, P.; Dunitz, J. D. *Acta Crystallogr.* **1979**, *B35*, 2020.

(83) Daniel, D. M.; Leadbetter, A. L.; Mazid, M. A. *J. Chem. Soc., Faraday Trans. 2* **1981**, *77*, 1837.

(84) Edwards, J. W.; Kington, G. L. *Trans. Faraday Soc.* **1962**, *58*, 1323.

(85) Andrews, J. T. S.; Westrum, J., E. F.; Bjerrum, N. *J. Organomet. Chem.* **1969**, *17*, 293.

(86) Atkins, P. W.; de Paula, J. *Physical Chemistry*, 7th ed.; Oxford University Press: Oxford, 2002; p 822.

(87) Pascual-Ahuir, J. L.; Silla, E.; Tunon, I. *GEPOL93*. http://server.ccl.net/cca/software/SOURCES/FORTRAN/molecular_surface/gepol93/.

(88) Bondi, A. *J. Phys. Chem.* **1964**, *68*, 441.

(89) Cox, J. D.; Pilcher, G. *Thermochemistry of Organic and Organometallic Compounds*; Academic Press: London, 1970.

(90) Edwards, J. W.; Kington, G. L. *Trans. Faraday Soc.* **1962**, *58*, 1334.

(91) Tomasseti, M.; Curini, R.; DÁscenzo, G.; Ortaggi, G. *Thermochim. Acta* **1981**, *48*, 333.

(92) Ogasahara, K.; Sorai, M.; Suga, H. *Mol. Cryst. Liq. Cryst.* **1981**, *71*, 189.

(93) Turnbull, A. G. *Aust. J. Chem.* **1967**, *20*, 2059−2067.

(94) Frenkel, M.; Marsh, K. N.; Kabo, G. J.; Wilhoit, R. C.; Roganov, G. N. *Thermodynamics of Organic Compounds in the Gas Phase*, Vol. 2; Thermodynamics Research Center: College Station, 1994.

(95) *Computational Thermochemistry. Prediction and Estimation of Molecular Thermodynamics*; Irikura, K. K., Frurip, D. J., Eds.; ACS Symposium Series No. 677: Washington, 1998.